Journal of Zhejiang University-SCIENCE A (Applied Physics & Engineering)
ISSN 1673-565X (Print); ISSN 1862-1775 (Online)
www.jzus.zju.edu.cn; www.springerlink.com
E-mail: jzus@zju.edu.cn

Experimental and theoretical studies of laterally loaded single piles in slopes*

Ming-hui YANG, Bo DENG†‡, Ming-hua ZHAO

College of Civil Engineering, Hunan University, Changsha 410082, China

†E-mail: parl_d@126.com

Received July 11, 2019; Revision accepted Oct. 17, 2019; Crosschecked Oct. 23, 2019

Abstract: In this study, a series of small-scale laboratory model tests and numerical simulations was performed to investigate the lateral behavior of a single pile embedded in slopes and in horizontal ground. In the model tests, small-scale model piles were fitted with strain gauges around their surface at various depths, while the lateral deflections at the pile head were measured by dial gauges. A total of four sets of model pile tests was conducted with piles installed in model slopes of 0°, 30°, 45°, and 60°. The changes in pile head deflections and their bending moments with changes in pile location and the embedded length of the piles were analyzed by the finite element method (FEM). Subsequently, a new *p*-*y* curve (*p* denotes the soil resistance and *y* denotes the pile deflection) for a steep clay slope was developed based on those finite element analysis results, taking into account the influences of the declination of the slope and the position of the pile in the slope. The numerical results agree very well with those from a scale model pile load test and other full-scale pile load tests reported in the literature.

Key words: Pile foundation; Slope; Model test; Finite element method (FEM); Lateral load; *p*-*y* curve
https://doi.org/10.1631/jzus.A1900318 **CLC number:** TU473.1

1 Introduction

As opposed to the majority of pile foundations which are placed in horizontal ground, some piles are constructed in steep slope areas to sustain lateral loads, such as wind, earthquake, impacting forces, and lateral pressure caused by soil movement. These types of piles are referred to as passive piles and are commonly encountered in bridge abutments adjacent to approach embankments (Springman, 1989; Gabr et al., 2002), piles built to stabilize slopes (Viggiani, 1981; Poulos, 1995), and existing piles adjacent to excavations (Leung et al., 2000; Choy et al., 2007).

The behavior of the laterally loaded pile on a slope is clearly different to that of a pile located in horizontal ground because of the attenuation of forces acting on the pile on the slope side. Therefore, significant research efforts have been devoted to studying the impact of slope on the behavior of laterally loaded piles near a slope, by means of centrifuge tests (Mezazigh and Levacher, 1998; Brandenberg et al., 2005), scale model tests (Poulos, 1976; Ng and Zhang, 2001), and finite element methods (FEMs) (Chae et al., 2004; Georgiadis and Georgiadis, 2010, 2012; Zhou et al., 2017, 2018). It has been recognized that the effect of the slope on the lateral load capacity of piles is gradually reduced with increasing distance from pile to slope crest, until it disappears completely at a certain value, with the range of 5*D* (Poulos, 1976) to 8*D* (Nimityongskul and Ashford, 2010), where *D* is the pile diameter.

Analytical methods are essential for obtaining convenient formulas to satisfy the requirements of

‡ Corresponding author
* Project supported by the National Natural Science Foundation of China (No. 51678230)
ORCID: Ming-hui YANG, https://orcid.org/0000-0002-0773-4061; Bo DENG, https://orcid.org/0000-0002-4679-1165

engineering practice. Among various approaches, the *p-y* curve (*p* denotes the soil resistance and *y* denotes the pile deflection) method has been commonly used for analyzing piles under lateral loads. In it the soil is assumed as a number of independent springs, while the pile is replaced by an Euler-Bernoulli beam. Generally, the shape of the *p-y* curve and its magnitude are much influenced by variance in soils and in their stratification characteristics. Various types of *p-y* curve for different loading conditions and different soil types in horizontal ground have been developed by many scholars (Matlock, 1970; Reese and Welch, 1975; Gazioglu and O'Neill, 1984; O'Neill and Raines, 1991; Reese et al., 1997; Kodikara et al., 2010; McGann et al., 2011; Yang et al., 2011; Chang and Hutchinson, 2013). Nevertheless, the available *p-y* curve methods for piles near, or in, slopes are rare. Tang and Yang (2018) proposed a new *p-y* curve for analyzing the lateral behavior of piles embedded in rock slopes. Georgiadis and Georgiadis (2010, 2012) also developed a *p-y* curve for a pile near soil slopes based on the results from a refined 3D finite element analysis (FEA), which worked well for different soil properties and pile geometries, and allowed the effects of ground inclination and pile-soil adhesion also to be taken into consideration. The results showed that the effect of slope would diminish at a depth greater than 6*D* below the ground surface when the slope angle was 45°.

However, the *p-y* criteria proposed by Georgiadis and Georgiadis (2010, 2012) are appropriate for a laterally loaded pile placed near a slope rather than for a pile in a slope. Moreover, many bridge pile foundations are constructed in slopes so as to avoid causing damage to the hillside, as shown in Fig. 1a, and the idealized problem is presented in Fig. 1c. When compared with the case depicted in Fig. 1b, the lateral behavior of the loaded pile in a slope shown in Fig. 1c becomes more complex owing to the extra loading caused by the weight of soil at the opposite side of the slope. As expected, the effect of the declination and height of the slope, and even the length of pile embedded in slopes determined by its exact location, should be fully considered when exploring the reduction of soil resistance acting on the pile. However, acceptable solutions that could take account of all the influencing factors mentioned above have not so far been reported in the literature.

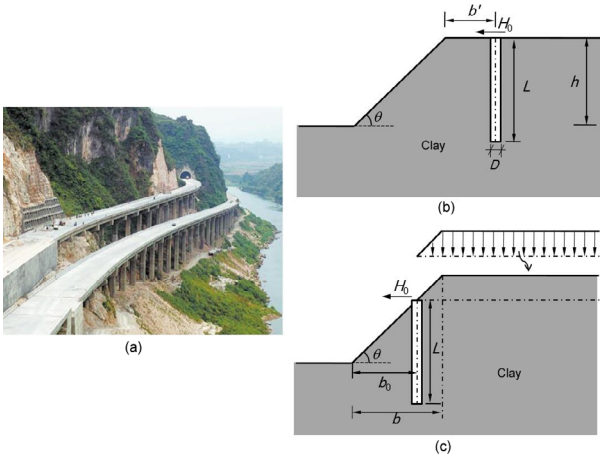

Fig. 1 Problem definition: (a) pile in a real-world slope; (b) model from Georgiadis and Georgiadis (2010, 2012); (c) model in this study (*L* is the length of pile; *h* is the slope height; *θ* is the slope angle; H_0 is the load at pile top; *b* is the horizontal distance from slope crest to slope toe; *b′* is the distance from pile top to slope crest; b_0 is the distance from pile cross section center to slope toe)

To address this problem, a number of small scale model tests were first carried out on model piles embedded in horizontal ground and in different slopes so as to investigate the behavior of laterally loaded piles. The lateral deflection at the pile head and the axial strains along the pile length were measured. The impact of slope on the lateral behavior of the piles was examined from the test results. In addition, numerical analysis was performed based on the finite element (FE) software ABAQUS (version 6.14.5) for examining various configurations, which had not been modeled in laboratory tests, i.e. pile location and pile length. A *p-y* curve analytical solution, based on these numerical results, was derived for a single pile embedded in a slope and subject to the lateral loading. Finally, a parametric study was conducted to investigate the lateral response of piles in slopes based on the proposed *p-y* curve.

2 Experimental investigation

2.1 Test tank and loading frame

A total of four laboratory model tests with different slope angles (*θ*), 0°, 30°, 45°, and 60°, were performed in a test tank, which was made of reinforced concrete with inside dimensions for length and

width of 4000 mm×2260 mm and with a depth of 1880 mm. The choice of these dimensions was to ensure that the tank could be separated into four parts by three monolithically constructed concrete boards (Fig. 2). To minimize any possible friction arising from the interface between the side walls and the soils, the test tank was covered with a film. Furthermore, a sufficient distance (>10D) from the boundary to the pile periphery was kept at 300 mm, so that boundary effects could be neglected (Matlock, 1970; Rao et al., 1996).

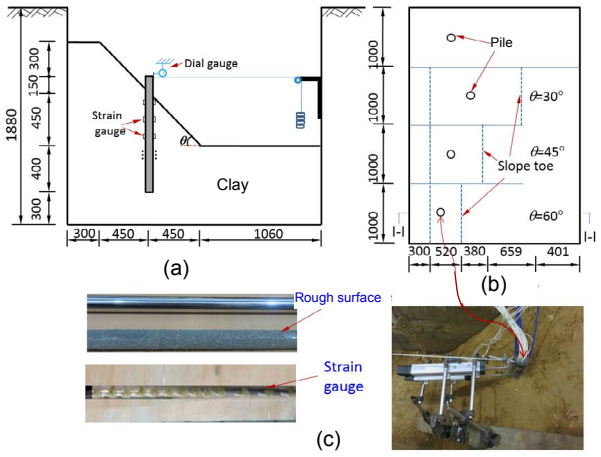

Fig. 2 Experimental setup (unit: mm)
(a) 1-1 side view; (b) Top view; (c) Arrangement of testing components

In model tests, lateral loads were applied by means of dead weight, and two dial gauges (0.01 mm) were used to record the pile head deflections. The details of the test instruments are shown in Fig. 2.

2.2 Soil preparation and pile installation

The model pile was made of aluminum alloy with outer diameter (D_p) of about 25.0 mm and wall thickness (d) of 1.0 mm. Its length (L) was 1.0 m while the free length (L_f) above the slope surface was 0.15 m. For consistency of test results, the dimensions and flexural rigidity (E_pI_p) of each pile were measured individually, and three-point bending tests (Timoshenko and Goodier, 1970) were adopted for obtaining E_pI_p. Furthermore, for simulating the pile-soil interface more realistically, the outside surface of each pile was abraded with some fine sand to form a circular rough contact surface (Fig. 2c). The ratio (β) of b_0 to b was set at 0.5, as indicated in Fig. 1c; the details of model parameters are shown in Table 1.

Table 1 Model test program

Case	$D_p \times d$ (mm×mm)	L (mm)	L_f (mm)	E_pI_p (N·m^2)	θ (°)	β
1	25.04×1.02	1000	150	100.85	0	0.5
2	25.06×1.04	1000	150	102.47	30	0.5
3	24.98×1.00	1000	150	102.35	45	0.5
4	25.01×1.03	1000	150	99.80	60	0.5

The experiments were carried out using commercially available clay with water content (W_c) of 26.6%, and an undrained shear strength (c_u) of 53.24 kPa. The clay was homogeneously compacted in layers of 150 mm by a wooden plate hammer, with the target dry unit weight being controlled to 14.45 kN/m^3. The above process was repeated until the required slope height and slope angle were achieved. During the slope model preparation, the pile was fixed by exerting a vertical load at the pile head and arranging a horizontal rope along the length of the pile at equal intervals when the height of clay reached 300 mm. Note that great care was taken to tamp the soil around the pile to ensure close contact between pile and soil. After waiting for 7 d to ensure the completion of the self-weight consolidation, the vertical load was removed and a lateral load was applied on the head of the pile in increments. Note that this method of pile formation is different from that used in practice, but this method has been adopted by many scholars (Chae et al., 2004; El Sawwaf, 2006), and good results have been obtained.

2.3 Measurement and loading arrangement

During the lateral load tests, the lateral deflections at the pile head, the axial strains along the pile length, and the lateral soil pressures were measured. Two dial gauges were used to measure the pile head deflections and their average was taken. Thirteen pairs of strain gauges were used to monitor the strain of the pile body and were installed in pairs along the model piles at various depths (Fig. 2c), so that the bending moment of the pile body could be evaluated by the axial strains. The exact locations of the testing components are shown in Fig. 2c.

All the static lateral loads were applied by increments of 0.1 kN, and increments were continued

until the rate of change of pile head displacement versus time was less than 0.01 mm/min or the cumulative rate of change was less than 0.1 mm/h. We repeated the above procedure until plastic failure of the soil in front of the pile occurred, that is to say when obvious cracks in the soil could be observed.

3 Results of model pile test and discussion

3.1 Pile head deflections

Fig. 3 depicts the measured pile head deflections in different slopes and in horizontal ground. Generally, the main distinction between the model pile in horizontal ground and in slopes is the lateral resistance of the upper parts of soil above the slope toe, so that the lateral load capacity of a single pile in level-ground is much greater than that for one in a slope. From Fig. 3, under the same lateral load, the greater the slope angle θ, the larger is the pile head deflection. This trend is more pronounced for a larger lateral load, indicating the significant effect of slope angle on the pile head deflections. This can be explained by the difference in the lateral resistance of soils in front of the piles for the three cases. For example, for a pile located in the middle of the slope in Fig. 3, the soil weight decreases with the increase of slope angle, thus the soil in front of the pile can provide less lateral resistance with a bigger slope angle. As such, it can be easily concluded that not only the slope angle θ, but also the distance b_0 (Fig. 1c), from the pile cross section center to the slope toe, can affect the lateral behavior of a loaded pile in slopes.

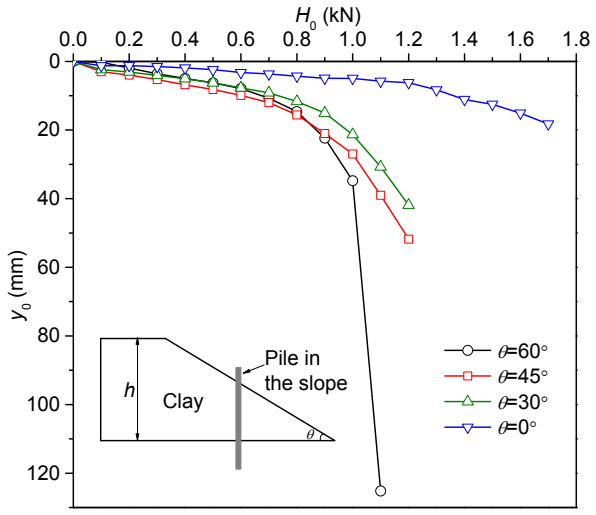

Fig. 3 Measured model pile head deflection for different θ under lateral loads (y_0 is the pile deflection at pile top)

3.2 Bending moments

Based on the measured strain values, the bending moments along the pile length can be calculated by

$$M = E_p I_p (\varepsilon_t - \varepsilon_c) / l, \quad (1)$$

where M is the bending moment of the pile body, l is the horizontal distance between the two gauges, and ε_c and ε_t are the compressive and tensile strains, respectively. This approach has been widely used by many scholars (Rollins et al., 1998; Ismael, 2010).

Because the distribution of bending moment along the pile length has a similar shape under different loading conditions, and in the case of a lateral load (P), for example, it reached 0.3 kN; the results are illustrated in Fig. 4. Apparently, regardless of the slope angle and even in horizontal ground, a similar trend can be found in the distribution of bending moment along the pile length. In other words, the bending moment in a pile always initially increases with the increase of pile depth, and then reaches the maximal value quickly. After that, the value of the bending moment will gradually diminish to zero at a certain depth and remain constant until the end of the pile. This trend coincides with the model test results conducted by Poulos (1976). Furthermore, it can be concluded that only the upper part of the soil surrounding the pile to a certain depth is mobilized, which is predominant in the lateral behavior of a loaded pile in slopes, but the soil resistance in the deeper part will be motivated when a larger lateral load is applied.

It is worth mentioning that the model pile used in laboratory tests was reduced in scale, whereas the clay used in the model was the same as that used in the prototype analysis. Thus, the model pile or the clay may not play the same roles as in the prototype because of scale effects. However, the main purpose of this study is to reflect the impact of slope angle on the pile response, and not to obtain a precise comparison between the prototype and model results. In addition, all the summaries above are based on a limited observation point along the piles. Therefore, to further understand the lateral-load behavior of a

single pile, analyses with more subtle changes of parameters are essential to develop the *p*-*y* curve method for piles in slopes. They will be discussed detailed in the next section by using FEM.

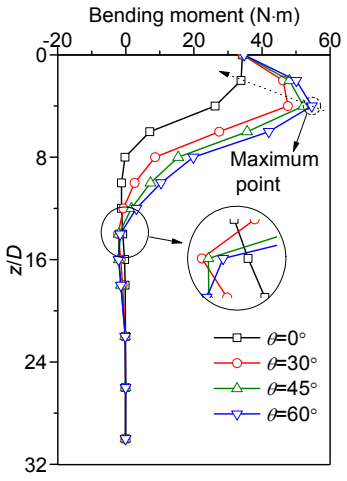

Fig. 4 Typical profiles of pile bending moment for *P*= 0.3 kN (*z* is the depth below ground surface)

4 Three-dimensional finite element analysis

4.1 Numerical results validation and discussion

Recently, by means of the ABAQUS program, Gupta and Basu (2016, 2017) and Wang et al. (2018) performed a series of 3D FE simulations for investigating the lateral behavior of piles. It is well recognized that FEM can provide a versatile tool for modeling pile-soil interface behavior. Thus, a series of FEAs were carried out to analyze the behavior of a laterally loaded pile located in a slope using the 3D non-linear computer program ABAQUS (version 6.14.5), in which model-scale piles were subjected to lateral loading with the same soil conditions as in the model tests.

A typical numerical model and 3D FE mesh are shown in Fig. 5, and the pile was modelled using 3D 8-node linear brick (C3D8) elements, whereas a 3D 10-node modified quadratic tetrahedron element (C3D10M) was used for the soil, and a refined mesh was used for the region of soil surrounding the pile and the soil close to the slope surface (the maximum mesh size ≤0.02 m). To reduce the boundary effect, a distance of more than 10*D* from the end of pile to the bottom of the model was set. Furthermore, the bottom of the soil model was fixed, and the normal displacements of the other four sides were fixed.

The Mohr-Coulomb model has been presented by many scholars (Miao et al., 2006; Georgiadis, 2014; Zhao et al., 2017; Wang et al., 2018) for capturing the failure and deformation characteristics of soils. Therefore, that constitutive model was used in this study to simulate the lateral responses of a pile constructed in a slope. The pile-soil interaction model also used the Coulomb friction model whose feasibility and accuracy have been well verified by many researchers (Miao et al., 2006; Rose et al., 2013; Haiderali and Madabhushi, 2016).

The FE calculations were conducted to simulate the lateral load behavior of a single pile and included four steps. Firstly, the initial stresses of the soil were generated through gravity loading without the pile. Then, the soil elements located at pile positions were replaced by pile elements. Next, the pile-soil interaction was simulated by using the contact interface element, which is a circular thin zone of 5 mm around the pile. Finally, an incremental lateral load was applied to the pile top.

To the authors' best knowledge, there has been little research reported on laterally loaded piles in slopes, and therefore the model test in this study was selected for the calibration of the numerical model. The input parameters used for validation are listed in Table 2. The undrained Young's modulus E_s and the undrained shear strength c_u for the test clay were obtained from undrained tri-axial tests, whereas the soil Poisson's ratio ν_s, the pile Poisson's ratio ν_p, and the interface friction coefficient μ_p were calibrated by the pile head deflections in the experiment with slope angle θ=30°. Note that the variations in μ_p would not affect the lateral pile response if gapping and slippage of the pile-soil interface were possible (Wang et al., 2018).

Fig. 6a shows a comparison between the pile head deflections obtained from the FEAs and those from the model test data. Similarly, a comparison of the distribution of bending moment is shown in Fig. 6b. Note that a constant Young's modulus in horizontal and vertical directions was used in the validation of the numerical simulation. Such a simplified method has been used by many scholars to compare the results of experimental and numerical calculations for the case of piles embedded in slopes

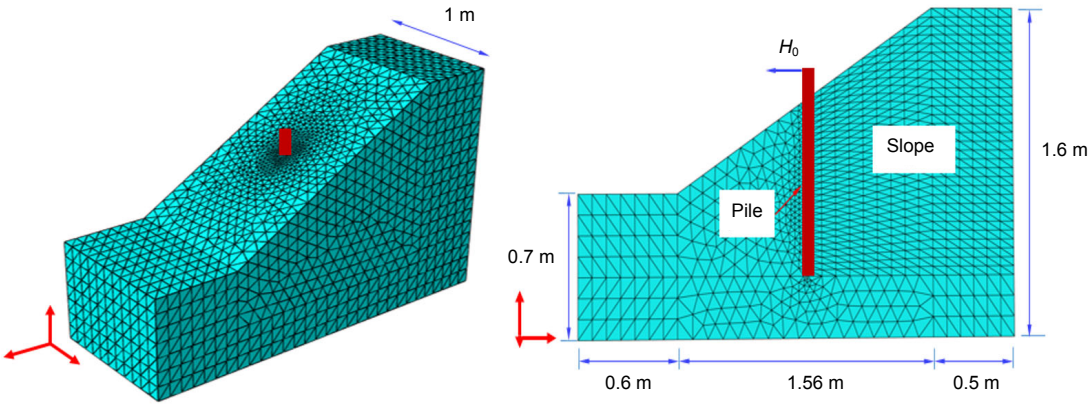

Fig. 5 Numerical model and 3D FE mesh for θ=30°

Table 2 Nonlinear finite element analyses

Case	L (m)	D (m)	θ (°)	β	γ_s (kN/m^3)	c_u (kPa)	E_s (MPa)	ν_s	γ_p (kN/m^3)	ν_p	μ_p
1	1	0.025	0, 10, 20, 30, 45, 60	1/2	18.3	53.24	30.12	0.35	25	0.2	0.5
2	0.7, 1.0, 1.5	0.025	30	1/2	18.3	53.24	30.12	0.35	25	0.2	0.5
3	1	0.025	30	x/24 (x=0–24)	18.3	53.24	30.12	0.35	25	0.2	0.5

γ represents the unit weight; subscripts p and s represent the pile and soil, respectively

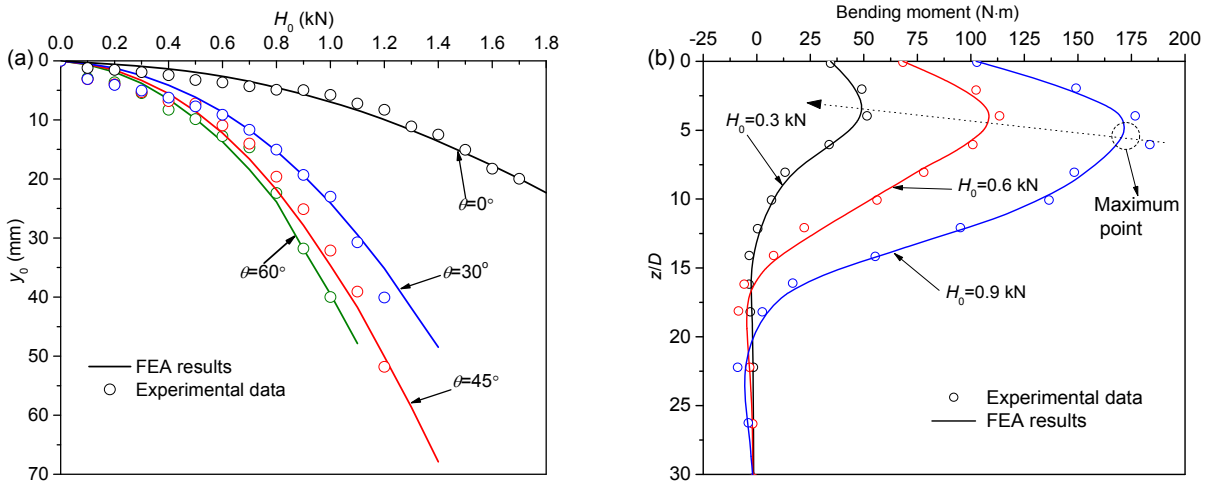

Fig. 6 Comparison of the test results with FEA: (a) deflection at pile top; (b) bending moment for θ=45°

(El Sawwaf, 2010; Lirer, 2012). Obviously, the FEA results fit well with the experimental results. That is to say, the FEA implemented in this study can provide a reasonable tool to predict the behavior of laterally loaded pile.

Typical computed results of the FEA are depicted in Figs. 7a and 7b for H_0=0.1 kN and 0.5 kN, respectively, which illustrate the effects of the slope angle and the pile location in slopes on pile behavior. As shown in Fig. 7a, the pile deflections increase with the increase of slope angle θ, especially near the pile top. However, the relationship in Fig. 7b between the pile location in the slope and its deflection is more complex. The deflection of the pile, which could reflect the soil resistance surrounding the pile, increases with increasing β at low values and reaches a maximum value when the pile is located at the exact middle of the slope, but then decreases when the

value of β varies from 0.5 to 1.0. It can be explained by the aggregated interaction effect of pile-soil in the upper and lower part of the pile embedded in the slope; the soil resistance at the upper part of the slope is dominant because of a larger value of b_0. Taking the pile A and pile B shown in Fig. 7b for example, pile A has a deeper embedded length compared with pile B, indicating that $b_{0a}<b_{0b}$, so that the soil provides more resistance for pile A. In such a case, the behavior of the lateral-loaded pile in the slope is similar to that of the anti-slide pile, and it has been found by previous researchers that the maximum possible safety factors for slope stability can be achieved if the anti-slide pile is placed at the exact middle of the slope so as to generate the maximum deflection of the pile (Cai and Ugai, 2000; Won et al., 2005).

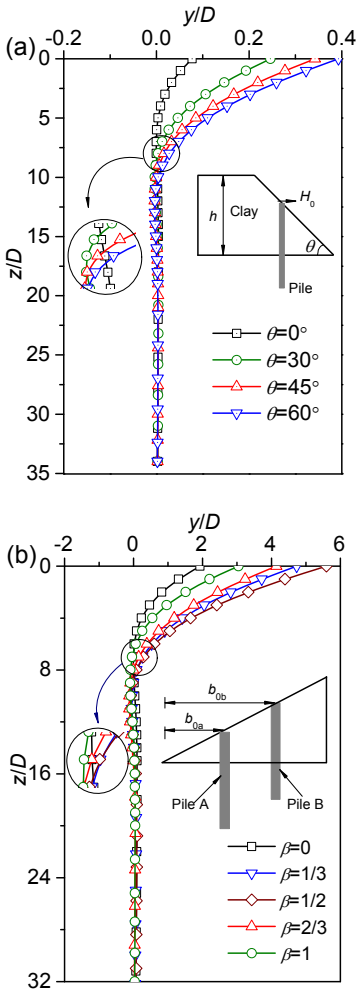

Fig. 7 Typical lateral deflection versus depth relationships from FEA for: (a) different θ at β=0.5; (b) different β at θ=45°

4.2 Development of *p-y* curves for a laterally loaded pile in a slope

A hyperbolic function of Kondner (1963) for constructing *p-y* curves has extensively been adopted to predict the behavior of the laterally loaded pile (Rajashree and Sitharam, 2001; Kim et al., 2004; Liang et al., 2009; Georgiadis and Georgiadis, 2010):

$$p=\frac{y}{1/K_{\mathrm{i}}+y/p_{\mathrm{u}}}, \tag{2}$$

where p is the lateral load per unit pile length (kN/m), y is the horizontal deflection of the pile (m), K_{i} is the initial soil stiffness (kPa), and p_{u} is the ultimate soil reaction (kN/m).

The ultimate lateral soil reaction p_{u} at depth z in Eq. (2) can be obtained from

$$p_{\mathrm{u}}=N_{\mathrm{p}}\times c_{\mathrm{u}}\times D, \tag{3}$$

where N_{p} is a bearing capacity factor that increases with depth. Obviously, K_{i} and N_{p} are the two critical parameters for determining the actual shape of the *p-y* curve.

The above value of N_{p} can be calculated from an empirical equation, and typically falls within the range of 3 to 9 (Matlock, 1970):

$$N_{\mathrm{p}}=\begin{cases}3+\dfrac{\gamma_{\mathrm{s}}z}{c_{\mathrm{u}}}+\dfrac{Jz}{D}, & z<z_{\mathrm{R}},\\ 9, & z\geq z_{\mathrm{R}},\end{cases} \tag{4}$$

where z_{R} is the depth of the reduced resistance zone, and J is a dimensionless coefficient that typically lies between 0.25 and 0.50.

Georgiadis and Georgiadis (2010) developed a *p-y* curve method for the lateral-loaded pile near a slope through a numerical analysis method and employed an empirical equation to take into account the effects of slopes on the value of N_{p}:

$$N_{\mathrm{p}}=N_{\mathrm{pu}}-(N_{\mathrm{pu}}-N_{\mathrm{po}}\cos\theta)\mathrm{e}^{-\lambda(z/D)/(1+\tan\theta)}, \tag{5}$$

where N_{po} and N_{pu} are the ultimate lateral bearing capacity factors for piles embedded in ground surface

and in deep lateral flow of soil, respectively, and λ is a dimensionless factor. The above three parameters can be determined by

$$\begin{cases} \lambda = 0.55 - 0.15\alpha, \\ N_{po} = 2 + 1.5\alpha, \\ N_{pu} = \pi + 2\Delta + 2\cos\Delta + 4\left(\cos\dfrac{\Delta}{2} + \sin\dfrac{\Delta}{2}\right), \end{cases} \tag{6}$$

where $\Delta=\sin^{-1}(\alpha)$, and α is the pile-soil adhesion factor which can be found in (Georgiadis and Georgiadis, 2010).

The initial stiffness of the p-y curve, K_i in Eq. (2) for laterally loaded piles in horizontal ground can be calculated by the following equation (Rajashree and Sitharam, 2001):

$$K_i = \frac{1.3E_{si}}{1-\nu_s^2}\left(\frac{E_{si}D^4}{E_pI_p}\right)^{1/12}, \tag{7}$$

where E_{si} and ν_s are the initial elastic modulus and Poisson's ratio of the soil, respectively, two of which can be obtained from tri-axial tests, E_p is the elastic modulus of the pile, and I_p is the inertia moment of the pile cross section.

A reduction factor μ is also used to account for the effects of slope on K_i (Georgiadis and Georgiadis, 2010):

$$\mu = \frac{K_{i\theta}}{K_{io}} = \cos\theta + \frac{z}{6D}(1-\cos\theta), \tag{8}$$

where K_{io} is the initial stiffness of the p-y curve for piles embedded in sloping ground, and $K_{i\theta}$ is the initial stiffness that can take account of the effect of θ on K_{io}.

As mentioned above, the developed p-y curve above is used to simulate the pile-soil interaction behavior of a lateral-loaded pile near a slope rather than actually in a slope, whereas this study aims at revealing the influence of the slope angle and the pile location on the p-y curve of a lateral-loaded pile in a slope; all the variable parameters for each performed analysis are summarized in Table 2.

4.2.1 Modification of N_p

The diagrams of p versus z for different lateral loads are derived by means of the second derivatives of the moment along the pile, so the p-y curves can be obtained by combining the p-z diagrams with y-z diagrams. For example, a typical p-y curve for different values of β and θ at the same depth are presented in Figs. 8a and 8b. From Fig. 8a, for a pile located at the toe of the slope, it can be seen that the horizontal ultimate bearing capacity reaches its largest value. However, it decreases as the pile location moves toward the midpoint of the slope until reaches a minimum at this point, and then it increases gradually when the location of pile moves toward the crest of the slope.

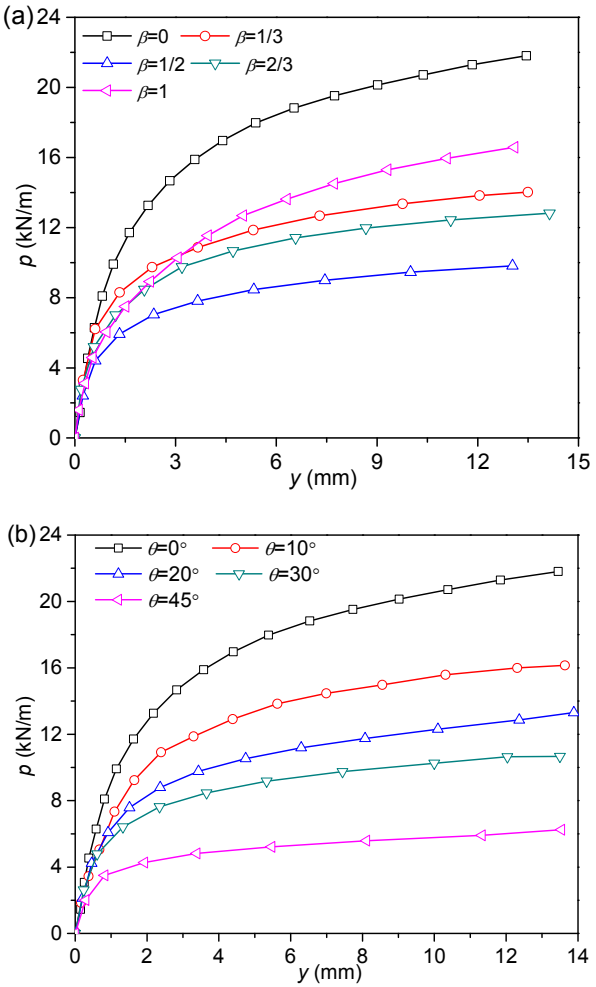

Fig. 8 Typical p-y curves derived from FEA for z=2D: (a) θ=30° and H_0=0.1 kN; (b) β=0.5 and H_0=0.5 kN

On the other hand, as shown in Fig. 8b, the ultimate lateral capacity of the pile decreases as the slope angle increases, and its value at slope angle θ=45° is only one-quarter of that in level ground. In this respect, a new p-y curve for lateral-loaded piles that are located in slopes should be proposed to take into account the effect of the slope, and another empirical equation of N_p based on Eq. (5) can be expressed as

$$N_p = N_{pu} - (N_{pu} - N_{po}\alpha_1^2\alpha_1^2)e^{-\lambda(z/D)\alpha_1^2}, \quad (9)$$

where α_1=1/(1+tanθ), α_2=1−sinθ(1+sinθ)/2. The variation of N_p with z obtained from Eq. (9), for the laterally loaded pile located in different slopes at β=0.5, is compared with the FEA results, as shown in Fig. 9, and good agreement can be obtained. It should be noted that c_u=29.8 kPa, which was obtained by fitting FEA results at θ=45°.

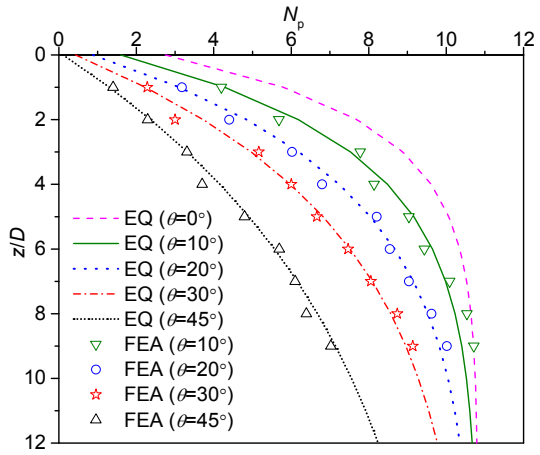

Fig. 9 Effect of inclination of slope on N_p versus z/D relationships

Furthermore, by taking the N_p–z/D data of laterally loaded piles that are embedded in the horizontal ground, located at middle of the slope, and at the slope crest as basic data, the relationships of N_p–z/D for the pile that located at any other point of the slope can be obtained. As illustrated in Fig. 10, the value of N_p can vary with β, and when β falls in the range of 0–0.5 or 0.5–1.0, the relationship of N_p with β is basically linear. As a consequence, the value of N_p can be approximately described by the following subsection functions:

$$\begin{cases} N_p = N_{pm} + \dfrac{1-2\beta}{N_{pg} - N_{pm}}, & 0 < \beta \le 0.5, \\ N_p = N_{pm} + \dfrac{2\beta - 1}{N_{pc} - N_{pm}}, & 0.5 < \beta < 1, \end{cases} \quad (10)$$

where N_{pg}, N_{pm}, and N_{pc} are the lateral bearing capacity factors when the pile is constructed in the ground, at the middle of the slope, and at the slope crest, respectively, and the values of N_{pg}, N_{pm}, and N_{pc} can be determined by Eqs. (4), (9), and (5), respectively. From Eq. (10), it can be seen that an amendment of N_p can take into account the effects of pile location in slope and slope angle simultaneously.

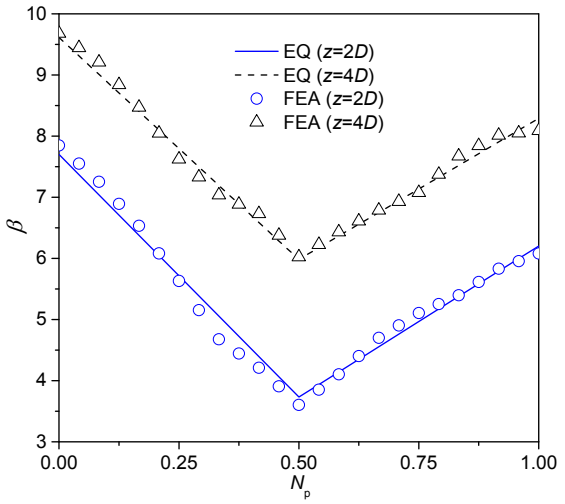

Fig. 10 Relationship of N_p versus β when z=2D and z=4D

4.2.2 Modification of K_i

The initial stiffness K_i for a laterally loaded pile represents the lateral soil resistance and depends on the coefficient of subgrade reaction K_s (Vesic, 1961). For a laterally loaded pile embedded in a slope, the soil surrounding the pile in a certain zone from the pile top to a critical depth defined as the reduction depth (denoted as h_0), cannot provide as much resistance as that in horizontal ground because of the limited width of soil, as shown in Fig. 11. However, the reduction of K_s and K_i will decrease with the increasing depth and vanish when the depth exceeds the value of h_0, where the values of K_s and K_i for a pile in slope can be equivalent to those of a pile in level ground. Therefore, FE analyses were conducted

to investigate the effect of the reduction caused by θ on K_i for sloping ground. As expected, the value of μ remained at 1.0 when the depth reaches a certain value related to the inclination of the slope, as shown in Fig. 11. According to the FEA results, the relationship between μ and θ can be obtained approximately from the following empirical equation:

$$\mu=\frac{K_{i\theta}}{K_{io}}=\cos\theta+\frac{z}{6D\tan\theta}(1-\cos\theta). \tag{11}$$

As compared with Eq. (8), the second term in Eq. (11) is used to consider the effect of the resistance of the upper parts of soil above the slope toe.

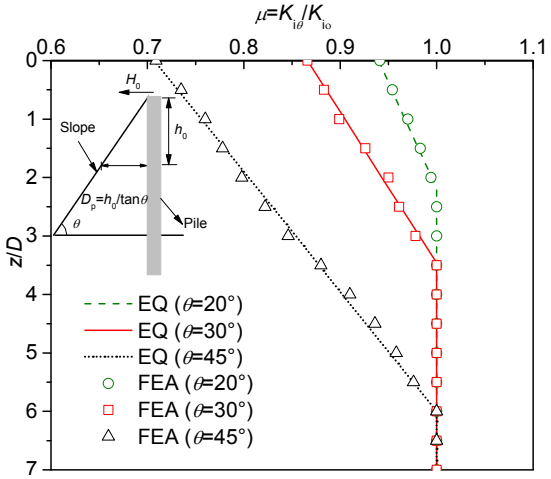

Fig. 11 Effect of slope angle on the reduction of K_i of the *p-y* curve (EQ indicates the result calculated by the proposed method)

5 Verification of numerical solution

Based on the proposed *p-y* curve discussed above, a program was developed in Matlab to carry out the calculation of the lateral-load-deflection of a single pile in a slope. The proposed numerical procedure was first verified against measurements from the laboratory model pile tests (Fig. 12). The pile-soil adhesion factor α equals 0.92 according to Fig. 9 plotted by Georgiadis and Georgiadis (2010), and the other parameters used for validation were as listed in Table 2, and thus the values of N_{pu} and N_{po} can be calculated as: N_{pu}=11.8, N_{po}=3.38. From these results, the calculated pile head deflections agree well with the model test data.

However, verification for the proposed *p-y* curve in a full-scale pile lateral loading test is also essential because of possible scale effects in the small-scale tests. As far as the authors are aware, no well-documented lateral loading test case exists, and thus the proposed method can be compared only with some special cases, such as the lateral loading of piles on level ground or near a slope.

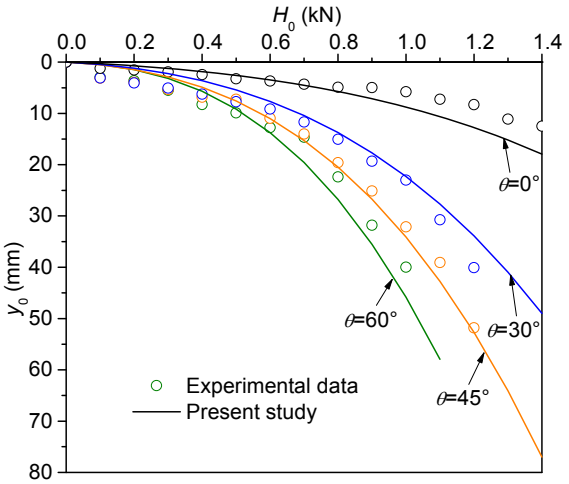

Fig. 12 Comparison of the measured and the calculated lateral displacements of the pile head for model test

The first full-scale load test (the Sabine test) for a pile located on level ground carried out by Matlock (1970) was examined. The pile has a diameter of D=0.319 m and the length L=12.8 m, E_pI_p=31 280 kN·m^2, E_s=2060 kPa, γ_s=5.5 kN/m^3, c_u=14.4 kPa, and α=1. Therefore, the values of N_{pu} and N_{po} can be obtained by the proposed method in this study and N_{pu}=11.94, N_{po}=3.5.

A second set of field tests for a pile that is located at the slope crest with a slope angle θ of 20° is used to validate the robustness of the proposed *p-y* curve method. It was conducted by Bhushan et al. (1979), and the parameters for verification were: D=1.22 m, L=5.185 m, E_pI_p=225 000 kN·m^2, E_s=24 440 kPa, c_u=220 kPa, γ_s=18.8 kN/m^3, and α=0.25. Therefore, N_{pu}=10.05 and N_{po}=2.38. Figs. 13a and 13b depict the measured and calculated pile head deflections under different lateral loading conditions, in comparison with the predicted results from the proposed *p-y* curve method, the analytical solutions of other researchers, and the measured data from the loading test. Good agreement is obtained between

these results. The proposed *p*-*y* curve method can thus provide a reliable tool for practical application in engineering.

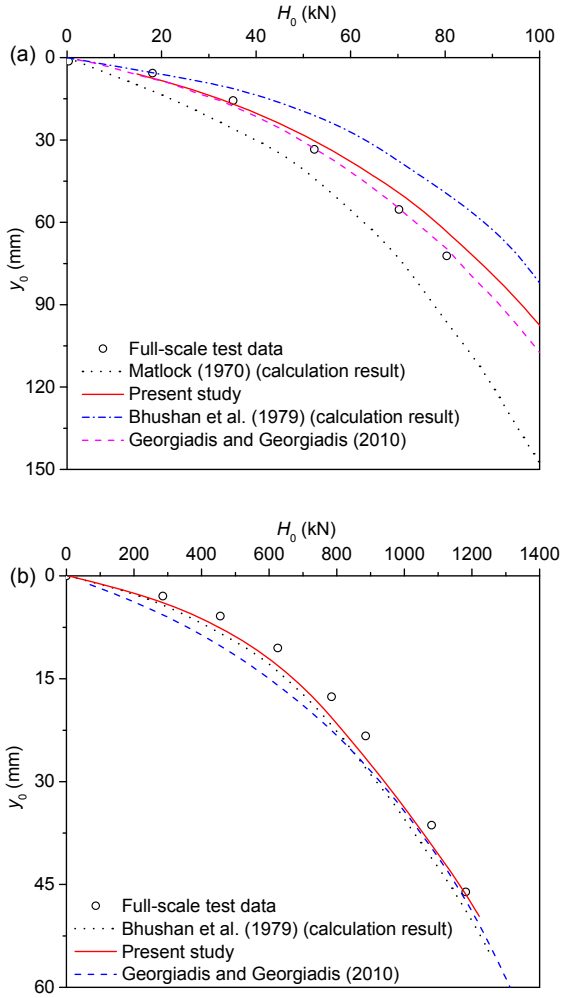

Fig. 13 Comparison of the measured and the calculated lateral displacements at pile top for full-scale tests from: (a) Matlock (1970); (b) Bhushan et al. (1979)

6 Parametric study

To investigate the effect of the pile locations and the slope inclinations on the ultimate lateral capacity of a single pile located in the base of the slope by the proposed *p*-*y* curve method, some numerical studies have been performed. Due to the important role of the pile length in the lateral behavior of the loaded pile, three pile lengths have been considered, namely 0.7 m, 1.0 m, and 1.5 m. All the other parameters are determined by the former model test.

Fig. 14 shows that the head deflection of lateral loaded piles in slopes varies with different values of the declination of the slope and the pile length. As a result, the pile head deflections increase as θ increases, and decrease with increasing pile length. For the pile (L=1.5 m) and an applied load (1.5 kN) for θ=30° and β=0.5, the value of the head deflection, y_0, is 12% larger than that of a pile in a slope of 20°. Meanwhile, the growth rate is 14% and 17% when L=1.0 m and 0.7 m, respectively. This trend can be explained by the shorter length of the pile, the less resistance caused by the soil, and the consequent greater increase in the deflection induced by the slope angle.

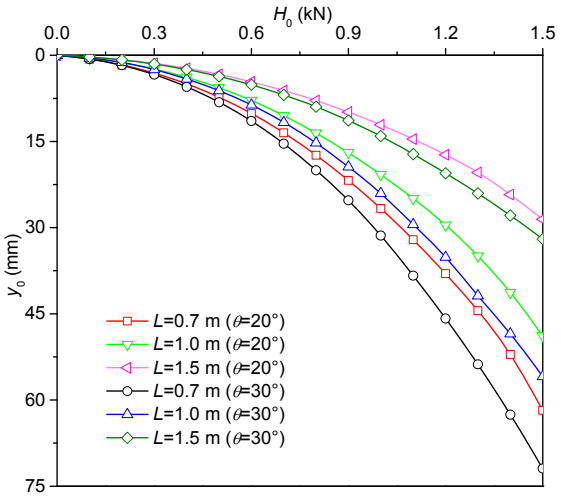

Fig. 14 Effect of ground slope on head deflection of pile with different pile lengths (β=0.5)

The results of the relationship between the pile location and the pile head deflection were shown in Fig. 15. From the results, the head deflection of the pile initially increases, and then decreases when the pile location moves from the slope toe to the slope crest. For the pile (L=1.5 m) with an applied load (1.2 kN) at β=0.5, the head deflection is 12.45 mm larger than that of a pile at β=1/6. Meanwhile, the pile head deflection decreases as the pile length increases under the same value of β. It indicates that the increase of head deflection of a pile caused by the location of the pile in a slope will be more obvious with a shorter pile.

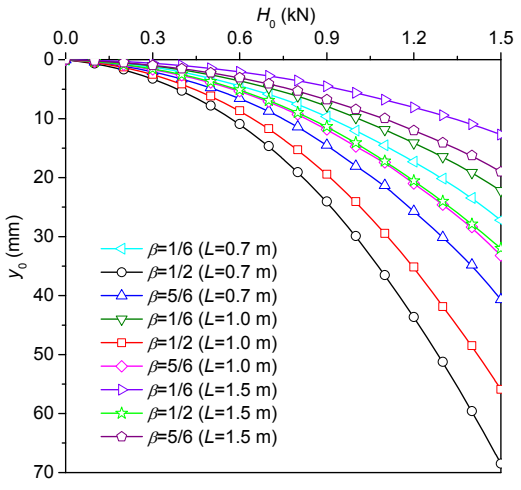

Fig. 15 Effect of position of pile in slope on head deflection of pile with different pile lengths (θ=30°)

7 Conclusions

This study investigates the lateral-loaded response of a single pile installed in the steep clay slopes commonly encountered in mountainous areas. To accomplish this goal, four sets of laboratory model tests and a series of 3D FE analyses for piles embedded in different slope angles and in level ground were conducted. Based on 3D FEA results, a new *p-y* curve is proposed to account for the effect of the pile location and the slope angle, which can be solved with a program developed by Matlab. The proposed *p-y* curve was verified by the results from laboratory tests and the full-scale lateral loading tests reported in previous literature. Therefore, the proposed *p-y* curve method can provide a reliable tool for practical application in engineering. Based on the results of this numerical and theoretical study, the following main conclusions can be drawn:

1. The distribution of the lateral deflection and the bending moment of a lateral-loaded pile in slope along the pile length are similar to those of pile embedded in horizontal ground. However, the slope inclination plays an important role in the lateral-load behavior of a single pile. A higher slope angle can cause a greater pile deformation and moment under the same loading conditions.

2. For piles with the same embedded length, the relationship between the ultimate lateral bearing capacity of the pile and the distance from the slope toe to the pile cross section center is approximately bilinear.

3. For the same pile with different embedded lengths, the ultimate lateral capacity of the pile increases linearly with increased distance from the slope toe to the pile cross section center.

Contributors

Ming-hui YANG wrote the first draft of the manuscript. Bo DENG performed the tests. Ming-hua ZHAO proposed the idea, supervised the research work, and revised and edited the final version.

Conflict of interest

Ming-hui YANG, Bo DENG, and Ming-hua ZHAO declare that they have no conflict of interest.

References

Bhushan K, Fong PT, Haley SC, 1979. Lateral load tests on drilled piers in stiff clays. *Journal of the Geotechnical Engineering Division*, 105(8):969-985.

Brandenberg SJ, Boulanger RW, Kutter BL, et al., 2005. Behavior of pile foundations in laterally spreading ground during centrifuge tests. *Journal of Geotechnical and Geoenvironmental Engineering*, 131(11):1378-1391. https://doi.org/10.1061/(asce)1090-0241(2005)131:11(1378)

Cai F, Ugai K, 2000. Numerical analysis of the stability of a slope reinforced with piles. *Soils Foundations*, 40(1):73-84. https://doi.org/10.3208/sandf.40.73

Chae KS, Ugai K, Wakai A, 2004. Lateral resistance of short single piles and pile groups located near slopes. *International Journal of Geomechanics*, 4(2):93-103. https://doi.org/10.1061/(asce)1532-3641(2004)4:2(93)

Chang BJ, Hutchinson TC, 2013. Experimental evaluation of *p-y* curves considering development of liquefaction. *Journal of Geotechnical and Geoenvironmental Engineering*, 139(4):577-586. https://doi.org/10.1061/(asce)gt.1943-5606.0000802

Choy CK, Standing JR, Mair RJ, 2007. Stability of a loaded pile adjacent to a slurry-supported trench. *Géotechnique*, 57(10):807-819. https://doi.org/10.1680/geot.2007.57.10.807

El Sawwaf M, 2006. Lateral resistance of single pile located near geosynthetic reinforced slope. *Journal of Geotechnical and Geoenvironmental Engineering*, 132(10):1336-1345. https://doi.org/10.1061/(asce)1090-0241(2006)132:10(1336)

El Sawwaf M, 2010. Experimental and numerical study of strip footing supported on stabilized sand slope. *Geotechnical and Geological Engineering*, 28(4):311-323. https://doi.org/10.1007/s10706-009-9293-9

Gabr MA, Borden RH, Cho KH, et al., 2002. *P-y* Curves for

Laterally Loaded Drilled Shafts Embedded in Weathered Rock. FHWA/NC/2002-08, North Carolina State University, Raleigh, USA.

Gazioglu SM, O'Neill MW, 1984. Evaluation of *P-Y* relationships in cohesive soils. Proceedings of Analysis and Design of Pile Foundations, p.192-213.

Georgiadis K, 2014. Variation of limiting lateral soil pressure with depth for pile rows in clay. *Computers and Geotechnics*, 62:164-174. https://doi.org/10.1016/j.compgeo.2014.07.011

Georgiadis K, Georgiadis M, 2010. Undrained lateral pile response in sloping ground. *Journal of Geotechnical and Geoenvironmental Engineering*, 136(11):1489-1500. https://doi.org/10.1061/(asce)gt.1943-5606.0000373

Georgiadis K, Georgiadis M, 2012. Development of *p-y* curves for undrained response of piles near slopes. *Computers and Geotechnics*, 40:53-61. https://doi.org/10.1016/j.compgeo.2011.09.005

Gupta BK, Basu D, 2016. Analysis of laterally loaded rigid monopiles and poles in multilayered linearly varying soil. *Computers and Geotechnics*, 72:114-125. https://doi.org/10.1016/j.compgeo.2015.11.008

Gupta BK, Basu D, 2017. Analysis of laterally loaded short and long piles in multilayered heterogeneous elastic soil. *Soils and Foundations*, 57(1):92-110. https://doi.org/10.1016/j.sandf.2017.01.007

Haiderali AE, Madabhushi G, 2016. Evaluation of curve fitting techniques in deriving *p-y* curves for laterally loaded piles. *Geotechnical and Geological Engineering*, 34(5):1453-1473. https://doi.org/10.1007/s10706-016-0054-2

Ismael NF, 2010. Behavior of step tapered bored piles in sand under static lateral loading. *Journal of Geotechnical and Geoenvironmental Engineering*, 136(5):669-676. https://doi.org/10.1061/(asce)gt.1943-5606.0000265

Kim BT, Kim NK, Lee WJ, et al., 2004. Experimental load-transfer curves of laterally loaded piles in Nak-Dong river sand. *Journal of Geotechnical and Geoenvironmental Engineering*, 130(4):416-425. https://doi.org/10.1061/(asce)1090-0241(2004)130:4(416)

Kodikara J, Haque A, Lee KY, 2010. Theoretical *p-y* curves for laterally loaded single piles in undrained clay using Bezier curves. *Journal of Geotechnical and Geoenvironmental Engineering*, 136(1):265-268. https://doi.org/10.1061/(asce)1090-0241(2010)136:1(265)

Kondner RL, 1963. Hyperbolic stress-strain response: cohesive soils. *Journal of the Soil Mechanics and Foundations Division*, 89(1):115-143.

Leung CF, Chow YK, Shen RF, 2000. Behavior of pile subject to excavation-induced soil movement. *Journal of Geotechnical and Geoenvironmental Engineering*, 126(11):947-954. https://doi.org/10.1061/(asce)1090-0241(2000)126:11(947)

Liang R, Yang K, Nusairat J, 2009. *p-y* criterion for rock mass. *Journal of Geotechnical and Geoenvironmental Engineering*, 135(1):26-36. https://doi.org/10.1061/(asce)1090-0241(2009)135:1(26)

Lirer S, 2012. Landslide stabilizing piles: experimental evidences and numerical interpretation. *Engineering Geology*, 149-150:70-77. https://doi.org/10.1016/j.enggeo.2012.08.002

Matlock H, 1970. Correlation for design of laterally loaded piles in soft clay. Proceedings of the 2nd Annual Offshore Technology Conference, p.577-594. https://doi.org/10.4043/1204-MS

McGann CR, Arduino P, Mackenzie-Helnwein P, 2011. Applicability of conventional *p-y* relations to the analysis of piles in laterally spreading soil. *Journal of Geotechnical and Geoenvironmental Engineering*, 137(6):557-567. https://doi.org/10.1061/(asce)gt.1943-5606.0000468

Mezazigh S, Levacher D, 1998. Laterally loaded piles in sand: slope effect on *P-Y* reaction curves. *Canadian Geotechnical Journal*, 35(3):433-441. https://doi.org/10.1139/t98-016

Miao LF, Goh ATC, Wong KS, et al., 2006. Three-dimensional finite element analyses of passive pile behaviour. *International Journal for Numerical and Analytical Methods in Geomechanics*, 30(7):599-613. https://doi.org/10.1002/nag.493

Ng CWW, Zhang LM, 2001. Three-dimensional analysis of performance of laterally loaded sleeved piles in sloping ground. *Journal of Geotechnical and Geoenvironmental Engineering*, 127(6):499-509. https://doi.org/10.1061/(asce)1090-0241(2001)127:6(499)

Nimityongskul N, Ashford S, 2010. Effect of soil slope on lateral capacity of piles in cohesive soils. Proceedings of the 9th US National and 10th Canadian Conference on Earthquake Engineering, article 366.

O'Neill MW, Raines DR, 1991. Load transfer for pipe piles in highly pressured dense sand. *Journal of Geotechnical Engineering*, 117(8):1208-1226. https://doi.org/10.1061/(asce)0733-9410(1991)117:8(1208)

Poulos HG, 1976. Behaviour of laterally loaded piles near a cut or slope. *Australian Geomechanics Journal*, G6(1):6-12.

Poulos HG, 1995. Design of reinforcing piles to increase slope stability. *Canadian Geotechnical Journal*, 32(5):808-818. https://doi.org/10.1139/t95-078

Rajashree SS, Sitharam TG, 2001. Nonlinear finite-element modeling of batter piles under lateral load. *Journal of Geotechnical and Geoenvironmental Engineering*, 127(7):604-612. https://doi.org/10.1061/(asce)1090-0241(2001)127:7(604)

Rao SN, Ramakrishna VGST, Raju GB, 1996. Behavior of pile-supported dolphins in marine clay under lateral loading. *Journal of Geotechnical Engineering*, 122(8):607-612. https://doi.org/10.1061/(asce)0733-9410(1996)122:8(607)

Reese LC, Welch RC, 1975. Lateral loading of deep foundations in stiff clay. *Journal of the Geotechnical Engineering Division*, 101(7):633-649.

Reese LC, Wang ST, Arrellaga JA, et al., 1997. LPILE Plus 3.0 for Windows. Ensoft, Inc., Austin, USA.

Rollins KM, Peterson KT, Weaver TJ, 1998. Lateral load behavior of full-scale pile group in clay. *Journal of Geotechnical and Geoenvironmental Engineering*, 124(6): 468-478. https://doi.org/10.1061/(asce)1090-0241(1998)124:6(468)

Rose AV, Taylor RN, El Naggar MH, 2013. Numerical modelling of perimeter pile groups in clay. *Canadian Geotechnical Journal*, 50(3):250-258. https://doi.org/10.1139/cgj-2012-0194

Springman SM, 1989. Lateral Loading on Piles Due to Simulated Embankment Construction. PhD Thesis, University of Cambridge, Cambridge, UK.

Tang XC, Yang MH, 2018. Analysis of laterally-loaded piles in weathered rock slopes based on *p-y* curve method. *International Journal of Geotechnical Engineering*. https://doi.org/10.1080/19386362.2018.1498199

Timoshenko SP, Goodier JN, 1970. Theory of Elasticity, 3rd Edition. McGraw-Hill, London, UK.

Vesic AB, 1961. Beams on elastic subgrade and Winkler's hypothesis. Proceedings of the 5th International Conference on Soil Mechanics and Foundation Engineering, p.845-850.

Viggiani C, 1981. Ultimate lateral load on piles used to stabilize landslides. Proceedings of the 10th International Conference on Soil Mechanics and Foundation Engineering, p.555-560.

Wang AH, Zhang DW, Deng YG, 2018. Lateral response of single piles in cement-improved soil: numerical and theoretical investigation. *Computers and Geotechnics*, 102: 164-178. https://doi.org/10.1016/j.compgeo.2018.06.014

Won J, You K, Jeong S, et al., 2005. Coupled effects in stability analysis of pile-slope systems. *Computers and Geotechnics*, 32(4):304-315. https://doi.org/10.1016/j.compgeo.2005.02.006

Yang EK, Choi JI, Kwon SY, et al., 2011. Development of dynamic *p-y* backbone curves for a single pile in dense sand by 1g shaking table tests. *KSCE Journal of Civil Engineering*, 15(5):813-821. https://doi.org/10.1007/s12205-011-1113-0

Zhao ZH, Li DY, Zhang F, et al., 2017. Ultimate lateral bearing capacity of tetrapod jacket foundation in clay. *Computers and Geotechnics*, 84:164-173. https://doi.org/10.1016/j.compgeo.2016.12.005

Zhou JJ, Gong XN, Wang KH, et al., 2017. A simplified nonlinear calculation method to describe the settlement of pre-bored grouting planted nodular piles. *Journal of Zhejiang University-SCIENCE A (Applied Physics & Engineering)*, 18(11):895-909. https://doi.org/10.1631/jzus.A1600640

Zhou JJ, Gong XN, Wang KH, et al., 2018. Effect of cemented soil properties on the behavior of pre-bored grouted planted nodular piles under compression. *Journal of Zhejiang University-SCIENCE A (Applied Physics & Engineering)*, 19(7):534-543. https://doi.org/10.1631/jzus.A1700118

中文概要

题　目： 边坡中单桩横向受力的试验与理论研究

目　的： 研究边坡段基桩的水平承载特性，以期指导工程实践。

创新点： 提出一种新的 *p-y* 曲线，以考虑边坡坡角和桩在边坡中位置的影响。

方　法： 1. 针对平地桩基和坡地桩基两种工况开展两组室内模型对比试验；2. 采用 ABAQUS 建立数值模型，并研究桩径、桩长和土体的弹性模量对桩基水平受荷性能的影响；3. 对室内模型试验结果和数值模拟结果进行对比分析，并得出坡地桩基的 *p-y* 曲线。

结　论： 1. 边坡中侧向受力桩的侧向挠度和弯矩沿桩长的分布与水平埋置桩的分布相似；然而，边坡倾角对单桩的侧向荷载特性有着重要的影响；在相同的荷载条件下，较高的倾斜角度会引起较大的桩身变形和弯矩。2. 对于埋置长度不变的桩，桩的极限侧向承载力与坡趾距桩截面中心的距离近似呈双线性关系。3. 对于埋置长度不同的桩，其极限承载力随坡脚至桩截面中心距离的增加呈线性增加。

关键词： 桩基；边坡；模型试验；有限元；水平荷载；*p-y* 曲线